Preparation of a Gold-Sputtered Optical Fiber as a Microelectrode for Electrochemical Microscopy

Guangda Shi,* L. F. Garfias-Mesias,* and W. H. Smyrl**

Corrosion Research Center, Chemical Engineering and Material Science Department, University of Minnesota, Minnesota 55455, USA

ABSTRACT

The preparation of microelectrodes for use in various electrochemical mapping techniques (e.g., scanning electrochemical microscopy and photoelectrochemical microscopy) is described. A commercial optical fiber (3.7 μm core diameter with 125 ± 2 μm and 245 ± 15 μm diam of cladding and coating, respectively) was stripped of its polymer coating at one end. The stripped core was then etched in different concentrations of hydrofluoric acid solution until a tip near 1 μm in diameter was achieved. The resulting optical fiber was coated with gold by dc-sputtering to produce a microelectrode less than 3 μm in total diameter. The optical fiber microelectrode was then coated with an insulating varnish yielding a final tip size normally less than 5 μm in diam. The final microelectrode was tested both for leaks in its polymer insulation and for electrical conductivity of the gold coating. The microelectrode has been used in several studies in our laboratories. Details of the preparation conditions are described here.

Introduction

Since the discovery of the scanning tunneling microscope (STM) by Binnig and Rohrer,[1] a number of different scanning microscopes has been developed, most of them using the original idea of moving a probe over a surface to get the desired properties of the substrate material or the characteristics of the interactions with its environment (normally liquid). Many research groups normally combine two or more of these techniques to study the microstructure and properties of different materials. In our laboratories the combination of scanning electrochemical microscopy (SECM) and photoelectrochemical microscopy (PEM) has been used together with scanning electron microscopy (SEM) and atomic force microscopy (AFM) to study the properties of titanium, aluminum, and other materials.[2] Most of the work on Ti has been done by using either the SECM[3-5,11] or the PEM.[5,6] Details of these techniques can be found in the literature.[5,6,8,9]

The SECM technique normally requires a microelectrode (usually less than 10 μm in diam) capable of supporting small currents generated by sensing species released by the local electrochemical reactions on the surface of the material. This microelectrode is isolated from the environment except at the tip, through which one measures the redox current generated by species released at electrochemically active sites on the sample surface. The most common materials used to prepare such tips are carbon fibers and platinum wires.[5,7] However, other metals can be used (i.e., gold or tungsten), provided that there is no interaction between the microelectrode and the surrounding system (for example, dissolution of the tip in aggressive environments).

The PEM technique, on the other hand, requires that light be focused or that it be provided by an optical fiber connected to a light source so that a small portion of the surface of a material is illuminated to generate a photoinduced electrochemical current.[8,9] Since the optical fiber is an electrical insulator, there is no need for additional coating. Furthermore, the tip is only used as a light source and does not take part in any measurement of photocurrent. Different sizes of optical fibers are commercially available. In our group we produce fiber tips with diameters that vary according to the specific studies.

In some cases, PEM and SECM can be combined to study the local reactions of materials like Ti.[5] To our knowledge, the smallest commercially available fiber optic to perform combined measurements of PEM and SECM is a 4 μm optical fiber core with an 80 μm gold coating and 125 μm polymer insulator. This means that although the resolution of the PEM experiment will be high (around 4 μm), the SECM experiment will have a poor resolution (around 80 μm). For example, the observation of inclusions[11] in polycrystalline Ti with these two techniques should depend on the size of the tip. A small tip allows both studies to be done with one scan with high resolution. One of the goals of our research has been the preparation of an optical fiber, sputtered with gold and insulated with a polymeric film that allows us to use it for PEM and SECM concurrently to produce images of the same area from a Ti sample. The main objective has been to produce a "thin" microelectrode with a total diameter smaller than 5 μm (2 μm or less for the optical fiber core, less than 1 μm thick gold ring, and about 2 μm thick polymer insulator), that could be used to determine the nature of the precursor sites for pitting in polycrystalline Ti.[11]

Experimental

Materials.—All solutions were prepared with 18 MΩ cm^{-1} deionized water with reagent grade compounds used without further purification. All the tip preparation and testing procedures were carried out at room temperature. Type F-AS optical fiber (3.7 μm core diameter with 125 ± 2 μm of cladding and 245 ± 15 μm of polymer coating) was obtained from Newport Corporation. Different concentrations of HF solutions were prepared from a concentrated 48% HF solution (Mallinckrodt). Potassium ferrocyanide ($K_4Fe[CN]_6$) was also obtained from Mallinckrodt. The insulating varnish (catalog no. 199-1480) was obtained from RS Components Corby, Northants, NN17 9RS, U.K.). The gold target (99.98% pure) used in the sputter coating was obtained from SPI Supplies. A series of 12, 1, and 0.3 μm polishing papers were used to polish the fiber tip.

Microelectrode preparation.—Fiber etching.—The optical fiber was cut into pieces that were approximately 1 m in length. The fibers were then stripped of their polymer coating with a fiber stripper (designed for fibers with coatings between 80 to 125 μm) at one end as shown in Fig. 1. The stripped end (about 5 cm long) was cleaned with isopropanol and then cleaved to ensure a flat surface at the fiber end. After the clean cleavage, the stripped fiber end was about 2 cm in length. The stripped end was then etched in 25 mL HF solutions in a plastic bottle with a plastic pipette fixed into the cap to support the fiber. In order to determine the time required to etch the fiber tip to a size of approximately 1 μm in diam, the cleaved fiber ends were immersed vertically into 5, 10, 20, and 48% (by volume) HF solutions. After completion of the etching period, the fibers were observed under 35 times stereoscope and the size of the fiber tip etched was estimated. The fibers used to establish the best preparation conditions were characterized in a SEM JEOL 840 II (with an integrated EDX system for X-ray analysis) or in a field-

* Electrochemical Society Student Member.
** Electrochemical Society Active Member.

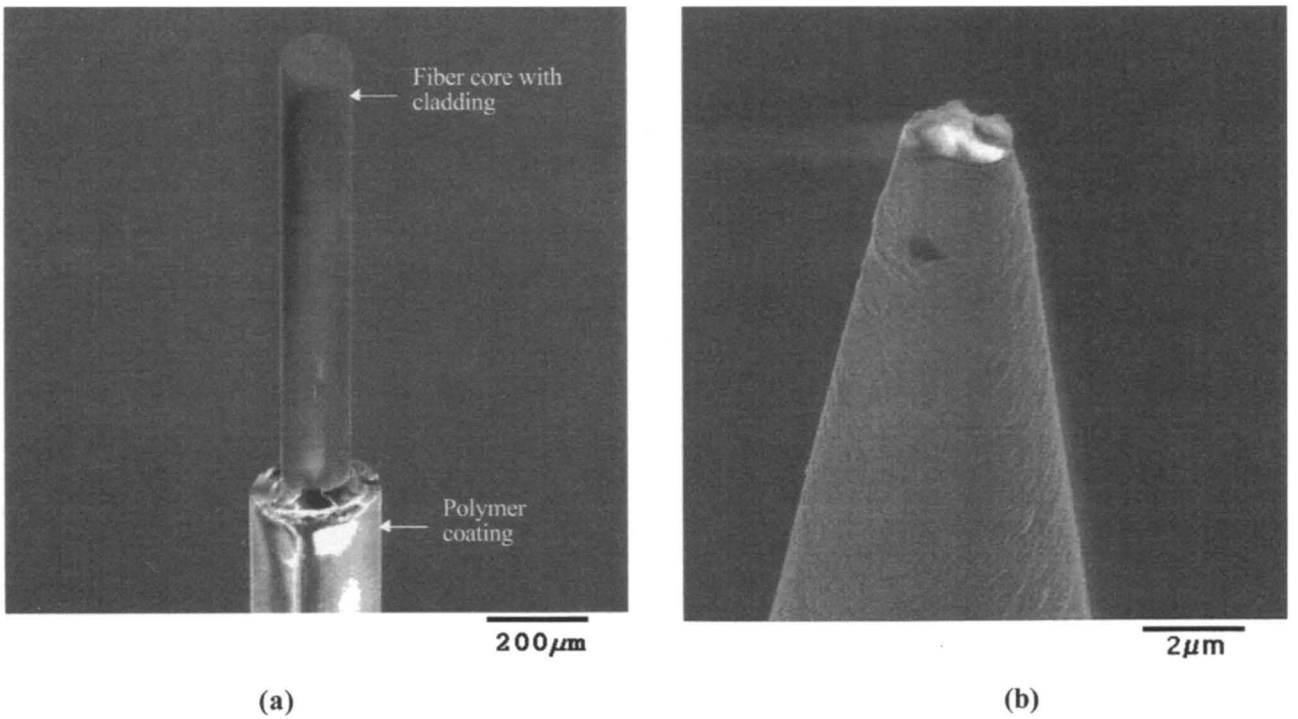

Fig. 1. (a) SEM image of a cleaved optical fiber; (b) SEM image of a fiber etched in 5% HF solution.

emission gun-scanning transmission electron microscopy (FEG-SEM) Hitachi S-800 (spatial resolution, 2 nm).

Gold sputtering.—After the etching process, the optical fibers were mounted and sputtered with high purity gold using a sputter coater (with etch mode) from SPI Supplies (U.S.) to produce the desired probe size. In order to achieve uniform gold thickness, the fibers were coated twice. The etched fiber was coiled onto a homemade support inside the vacuum chamber in one orientation during the first coating, and then in a second orientation during the second coating. The fiber was coiled horizontally to ensure an equal distance along the fiber with respect to the gold target. The thickness of the gold coating was controlled by adjusting the fiber distance from the gold target, the coating current density, or the coating time. In our setup, the fiber was placed 1.5 to 2 cm from the gold target and coated for 8 min with a current density of 18 mA. It was then coiled again in the reverse direction and coated for another 8 min using the same current density.

Insulating polymer coating.—For SECM studies, it is required that the gold coating has to be insulated except at the end of the fiber tip. This was accomplished by dipping the gold-coated etched fiber into an insulating varnish (RS Components, U.K.). The tip was then left to dry for 1 h or more. This procedure was normally repeated three times to ensure a good insulation. However, some microelectrodes required further coatings, if they were not well insulated. Furthermore, it was observed that if the microelectrodes were left to dry overnight, they tended to be better insulated.

Sanding and polishing.—After the insulating varnish was completely dried, a few fiber tips were completely covered (those with tip diameter larger than 2 μm, as discussed below), and therefore it was necessary to remove the varnish at the end of the tip to expose the fiber and the gold ring so that both light and current could be conducted through the assembled tip. In order to remove the gold on the end of the tip, a 12 μm Al_2O_3 lapping paper was used to sand lightly the end of the optical fiber (disk) and the gold sputtered ring. The polishing steps were accomplished by fixing the fiber tip into an X-Y micropositioner (see Fig. 2), parallel to the x axis, and then moving the microelectrode in the y direction with the tip perpendicular to the polishing paper. In addition, a low power red laser was used to pass light through the optical fiber. This procedure was repeated under observation in the 35 power stereoscope until the red laser light could be observed at the end of the fiber tip illuminating the lapping paper. Once the fiber tip was opened, it was further polished using the same method, with 1 and 0.3 μm size lapping paper.

Results and Discussion

The preparation conditions described above are an inexpensive way for producing microelectrodes that can be used for various applications in research. The microelectrodes obtained using this method were characterized step by step with different techniques. Observation of the etched fiber tips showed that more dilute (5%) HF solutions tend to yield the best tips despite the fact that it takes a longer time to fully etch them. Use of the more concentrated HF solutions (48 and 20%), required precise timing (about 1 to 2 h); otherwise, the tip could be etched away completely. In addition, the more concentrated HF solutions did not produce sharp tips but long thin tips that are uniformly small. Although the latter tips were sufficiently small, they were not suitable for scanning because they were extremely weak and fragile. We observed that it takes approximately 20 h to produce the finest fiber tip when a 5% (by volume) HF solution is used. A SEM image of a well-etched optical fiber is shown in Fig. 3. The fiber end was less than 2 μm diam with a sharp end (see Fig. 3a). Since the final diameter of the fiber was sufficiently small for our tests, most of the following steps (gold coating, insulating polymer coating, and sanding) were further investigated using these small tips.

Following the fiber etching, the deposition with gold on the end part of the fiber was easily accomplished. Figure 4 shows typical etched fibers sputter coated with gold. The gold was found to be evenly distributed on the surface of the fibers. It was observed that the etched tips smaller than 2 μm in diam were only partially covered with gold at the end of the tip (Fig. 4b and c). However, tips with larger diameter (above 2 μm) were fully covered with gold (Fig. 4a). This behavior is not fully understood at this time. One possible explanation may be that the smaller tips do not have sufficient surface area for the gold to achieve good adhesion onto the fiber. Further work will aim to determine the cause of this finding.

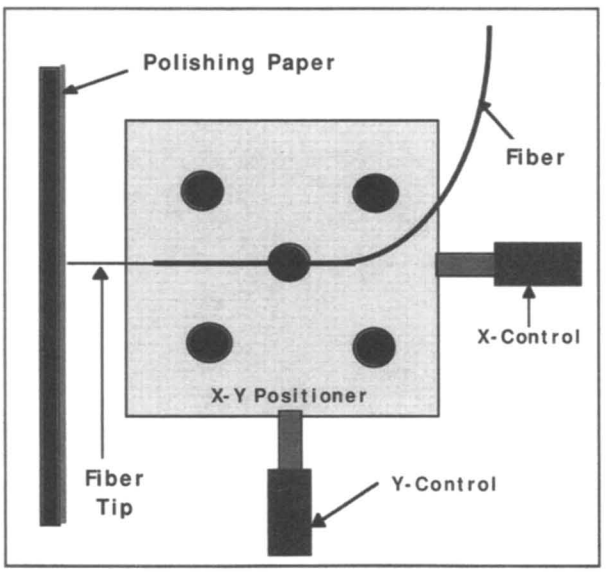

Fig. 2. Schematic representation of the X-Y micropositioner (top view).

Electrical conductivity of the gold coating was tested by using a Multimeter (Fluke 70 Series) and measuring the resistance between the two ends of the gold coating. To avoid damage to the electrode during testing, the sides of the fiber coated with gold were sandwiched inside small pieces of aluminum foil, then the probes of the multimeter were clamped onto the aluminum. In all gold-sputtered microelectrodes, the resistance was usually lower than 0.1 Ω, only very few of them had discontinuities in the gold coating. The discontinuities usually are located at the stripping point of the fiber tip and at the places where the fiber was held during the sputtering. In those cases, the microelectrodes were again placed inside the sputter coater and more gold was deposited with the same conditions described above. Usually, less than 1 μm thick gold coating was sufficient to ensure good conductivity along the optical fiber.

After the gold deposition on 50 to 75% along the fiber, the end of it was insulated (approximately 10 cm). Figure 5 shows the SEM image of three different insulated microelectrodes. Figure 5a shows a microelectrode whose tip diameter was small (just larger than 1 μm). Just as in the case of the gold sputtering, the insulating varnish did not coat the end of the tip. However, as it can be seen in Fig. 5b, a microelectrode with a tip diameter of about 2 μm was totally covered with the insulating varnish and therefore it had to be polished down. Notice the scratches and "damage" that were caused by polishing with the lapping paper. Finally, Fig. 5c clearly shows the top view of a microelectrode with its gold ring and insulating polymer; notice the flatness of the optical fiber end and the columnar deposition of the gold. Some pileup of the polymer was observed

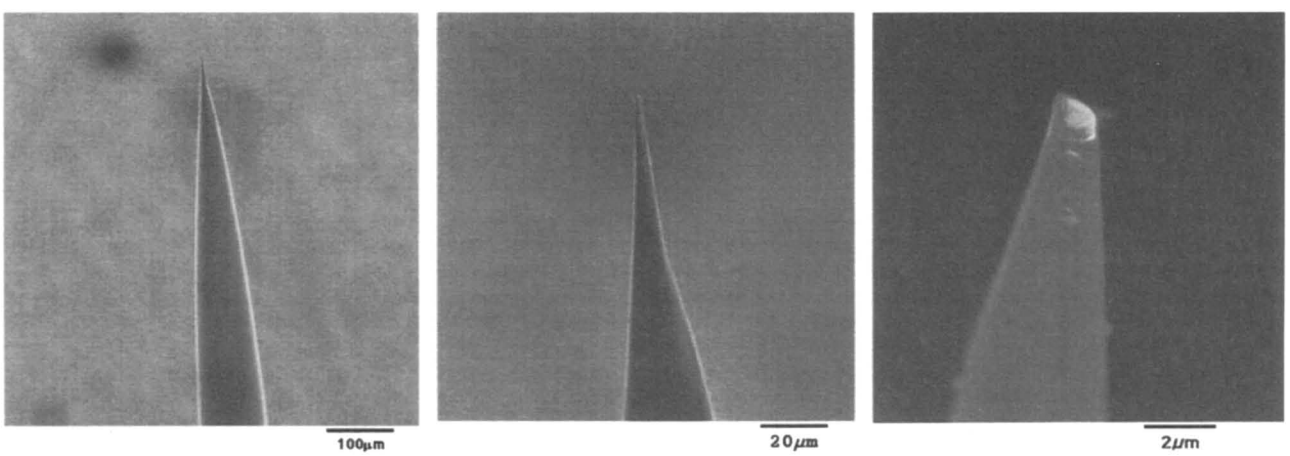

Fig. 3. SEM images of an etched optical fiber tip at different magnifications.

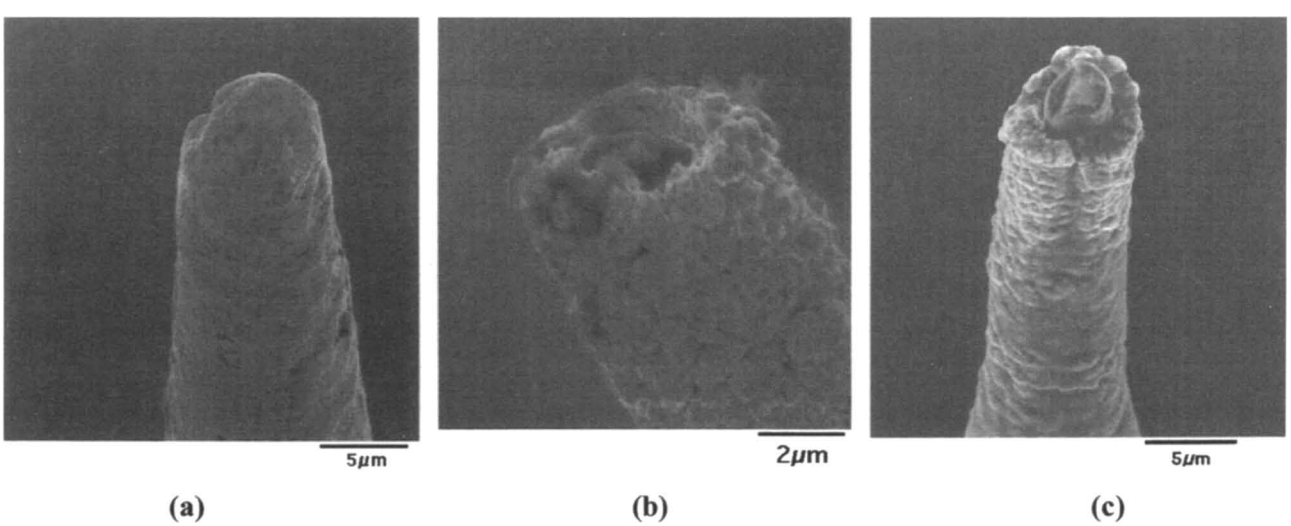

Fig. 4. Close up SEM image of gold coated optical fibers.

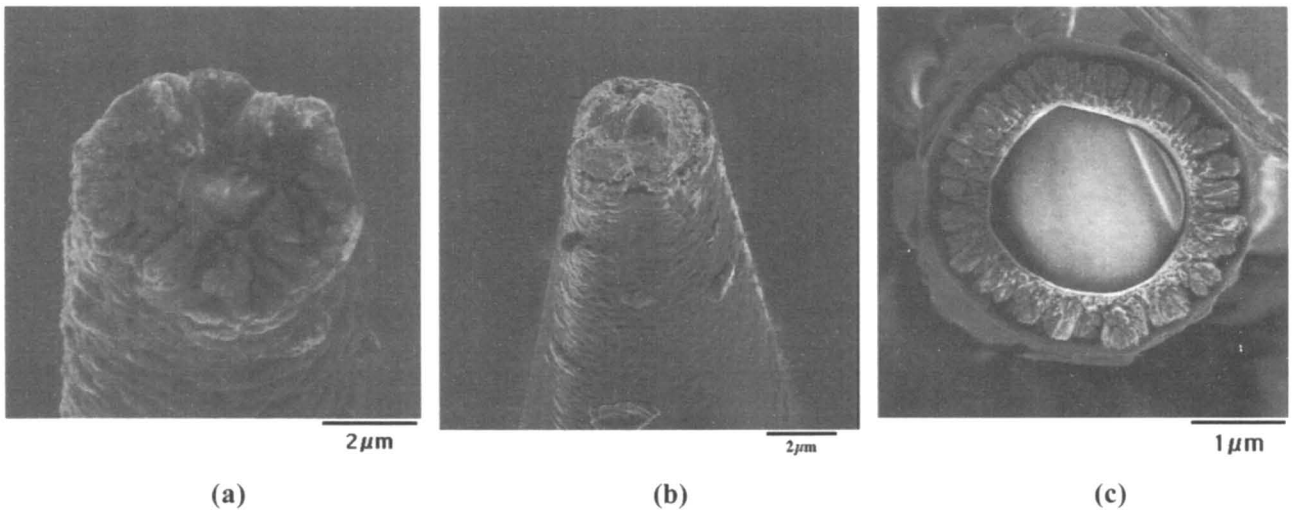

Fig. 5. (a) SEM image of a gold sputtered fiber tip that has been insulated with the varnish (open at the end); (b) SEM image of a polished fiber tip; (c) SEM image of top view of a fiber tip.

far from the tip. This was normally reduced by pulling the tip from the insulating polymer slowly.

Once the insulating material was dried, the tip was then tested in a 0.1 M $K_4Fe(CN)_6$ solution using a standard three-electrode cell configuration (WE = finished microelectrode, RE = standard calomel electrode, and CE = Pt wire). The voltammetric response (50 mV/s) of a typical well-insulated microelectrode is shown in Fig. 6. In a well-insulated tip the current is constant and well below 1 nA (when the tip is completely insulated). However, when measuring this level of current the signal is rather noisy and fluctuations around that value could be observed (as shown in Fig. 6).

The microelectrodes that have a tip diameter below 3 μm after the coating and those "larger" microelectrodes which have been opened in the tip (by sanding the end, as described above), were tested in the same solution described above. In most cases, after gold coating the thinner tips (less than 3 μm diam), it was observed that they were coated evenly, except at the very end of the tip (within the final 0.5 μm) where the gold ended. The larger microelectrodes were illuminated with an argon ion laser (351 nm wavelength and about 40 mW), and the insulating polymer (already dried) in the end of the tip was normally removed. However, some of these microelectrodes (with thicker insulating coating at the end of the tip) had to be sanded down by using the procedure described earlier. Figure 5b shows the tip of a microelectrode polished with three different size lapping papers after coating with the insulating varnish. The diameter of the optical fiber in this case was less than 1 μm, the gold coating was about 1 μm thick, and the insulating polymer approximately 0.5 μm yielding a final tip diameter of about 3.5 μm. In all optical fiber microelectrodes prepared with this procedure, the final diameter was normally between 3 and 5 μm. After ensuring that both the fiber disk and the gold ring on the end of the tip were exposed, the microelectrode was tested. The optical fiber was tested by illuminating one end of the fiber with the laser; by observing the light at the end of the tip it was possible to determine if the fiber was ready for PEM testing.

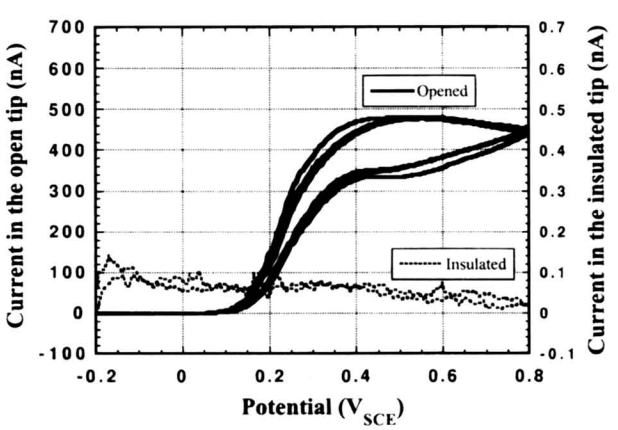

Fig. 6. Cyclic voltammogram of two different microelectrodes, one that is fully insulated, and one that is open just at the apex of the fiber probe.

The gold portion of the microelectrodes was tested in the potential range between −200 and 800 mV against the SCE; a typical voltammogram is shown in Fig. 6. In this case, the value of the diffusion-limited current (I_d) is around 450 nA. However, this value was not the same for all microelectrodes and was found to be in a "wide" range of current between 200 to 500 nA. These values were compared with theoretical calculations using the equations described by Szabo[12] and Smythe[13] for ring microelectrodes. A more detailed description and discussion regarding thin ring microelectrodes can be found in different publications cited in Ref. 14. According to most of the authors,[14] the equation proposed by Smythe[13] is the most accurate for defining the diffusion-limited current of a thin ring microelectrode.

Smythe[13] introduced the following expressions to calculate the steady-state diffusion current as

$$I_d = nFDCl_o \quad [1]$$

$$l_o = \frac{\pi^2(a + b)}{\ln[16(a + b)/(b - a)]} \quad [2]$$

where n is the number of electrons; F is the Faraday constant 96,485 C/mol; D is the diffusion coefficient, (0.739×10^{-5} cm^2/s); C is the concentration of electroactive species, 0.1 mol/L; a is the inner ring radius; and b is the outer ring radius.

Unfortunately in the case of the microelectrodes shown here, they do not fulfill the main condition established by the equations, which determine a "thin ring" as having a ratio of $a/b > 0.91$ (in our calculations we assumed a ring of approximate 1 μm internal diameter and 2 μm external diameter having $a/b = 0.5$). Nevertheless, assuming that the equation is still valid for these microelectrodes, the calculated current was around 9 nA. Obviously, this value is about twenty times smaller than the experimental values measured and described above.

The equations described by Szabo[12] to calculate the diffusion-limited current are relatively more convenient to describe the behavior of these microelectrodes, since the

conditions imposed are fulfilled by the dimensions of the microelectrodes. The most important equations are

$$I_d = nFDCl_o\left[1 + \frac{l_o}{(4\pi^3 Dt)^{1/2}}\right] \quad [3]$$

where t = time elapsed and l_o can be described for either $(b-a)/b << 1$ as

$$l_o = \frac{\pi^2(a + b)}{\ln[4e^{3/2}(a + b)/(b - a)]} \quad [4]$$

or for any ring microelectrode with different thickness as follows

$$l_o = \frac{\pi^2(a + b)}{\ln[32a/(b - a) + \exp(\pi^2/4)]} \quad [5]$$

Taking the expressions to calculate l_o one can estimate the value of the expected limiting current. In both cases the value was close to 27 nA, which is still much smaller than the experimental value obtained. The discrepancy between the calculated values and the experimental limiting current can be explained by the combination of three different factors (described below in order of relevance)

1. The porosity of the gold ring. As shown in Fig. 5, the gold ring is far from having a flat surface. It is more likely that the roughness of the deposited gold increases the surface area of the gold and therefore the real area exposed to the environment is higher than that of a conventional (and well polished) ring electrode.
2. As described before, the insulating varnish does not cover completely the apex of the microelectrode, and as a consequence, the real exposed area goes beyond a flat ring but rather is a shallow cylinder.[7]
3. Finally, it is important to remember that although the lacquer has a very low conductivity, once it dries, there may be pinholes that expose the electrode. These can also contribute to the overall current measured.

From the authors' point of view, it is more likely that the surface roughness and the complexity of the shape of the exposed gold ring microelectrode can substantially increase the limiting current by increasing the total area exposed to the electrolyte. Pores and holes in the varnish may contribute to the higher limiting currents but it is very unlikely that this can be the main explanation because of the relatively thick coating applied to the microelectrode.

Smaller tips can be obtained and will be discussed in future work. On the other hand, larger tip diameters could also be obtained but they are inherently detrimental for the purpose of our research. Although the current measured during SECM tests would be increased, it would illuminate a larger region of the sample and therefore would decrease the resolution of the electrochemical images.

The method used here to prepare the microelectrodes yielded robust microelectrodes with some features that suggested that they can be used in a wide variety of applications. The microelectrodes are currently being used in our laboratories, and we have already observed that they are stronger than the normal optical fiber. For example, they are easier to handle than commercial optical fibers (which break easily when accidentally contacted with the surface of the sample). The microelectrodes resist relatively gentle crashes, probably because both the gold coating and the varnish helps to prevent premature damage of the tip. It is also important to mention that it takes approximately 2 days to prepare one batch of microelectrodes, but since a batch of ten or more can be prepared at the same time, it is clearly an easy way to produce them.

Figure 7 shows the SEM image of an inclusion in a sample of polycrystalline titanium (a) together with the PEM image of the same grains (b) where the grain structure can be clearly seen. Furthermore, some topographic information can also be obtained by using this microelectrode. Finally, the image in Fig. 7c shows the SECM of the same area showing the area with higher electrochemical activity (darker) and the area that surrounds the particle. Both images (PEM and SECM) were obtained with the same microelectrode and apart from facilitating the measurement, the lateral resolution of the images was quite satisfying.

Conclusions

A method for producing microelectrodes for testing reactive surfaces has been developed. The microelectrodes are

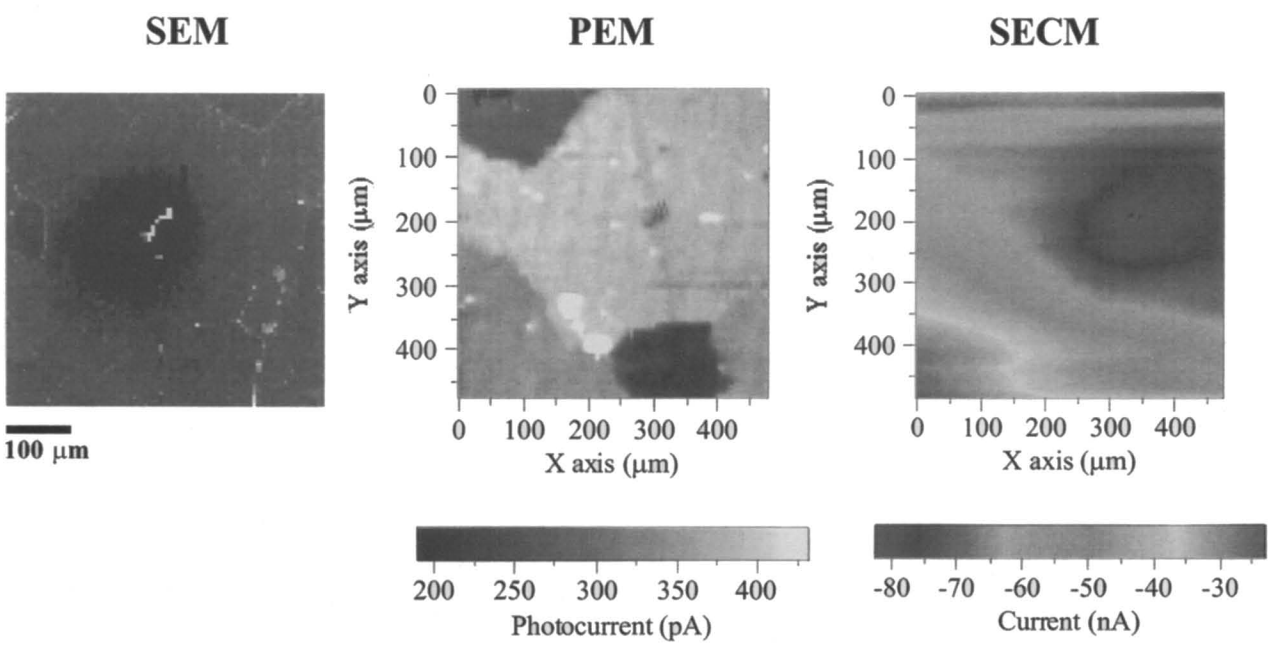

Fig. 7. SEM, PEM, and SECM of the same area in a large grain Ti sample containing an inclusion (Al-Si particle). Notice the inclusion appearing as a dark area inside the grain shown in the PEM image (b, center) and then shown as a region of high electrochemical activity in the SECM test (c, right). The PEM image was done in a 0.05 M H_2SO_4 solution, the Ti electrode was polarized at +1.5 V_{SCE} (the total current measured in the Ti electrode was 48 nA). The SECM image was obtained by using a 0.1 M $K_4Fe(CN)_6$ solution, the Ti electrode was biased at 1 V_{SCE} (the total current measured in the Ti electrode was 8.5 A), whereas the gold part of the microelectrode was biased to 0 V_{SCE} (the background current measured in the microelectrode in this solution prior to biasing the Ti electrode was 120 pA).

mainly for PEM and SECM measurements but may be used in other applications. It was possible to achieve microelectrodes with an optical fiber core diameter of 1 to 2 μm and a thin layer of gold that yields microelectrodes with an approximate size of 3 μm. Further insulation resulted in a total tip diameter less than 5 μm. The microelectrodes produced by the method described here had excellent and improved resolution for both PEM and SECM images. Future work is in progress to use optical fiber microelectrodes to perform PEM and SECM concurrently.

Acknowledgments

This study was supported by NSF grant DMR-9509766. The authors would like to thank Dr. T. Momma for his help with the FEG-SEM and Dr. P. I. James for his valuable discussion.

Manuscript submitted November 4, 1997; revised manuscript received February 3, 1998.

The University of Minnesota assisted in meeting the publication costs of this article.

REFERENCES

1. G. Binnig and H. Rohrer, *Helv. Phys. Acta*, **55**, 726, (1982).
2. J. P. H. Sukamto, W. H. Smyrl, N. Casillas, M. Al-Odan, P. James, W. Jin, and L. Douglas, *Mater. Sci. Eng. A*, **198**, 177, (1995).
3. N. Casillas, S. Charlebois, W. H. Smyrl, and H. White, *J. Electrochem. Soc.*, **140**, L142 (1993).
4. N. Casillas, S. Charlebois, W. H. Smyrl, and H. White, *J. Electrochem. Soc.*, **141**, 636 (1994).
5. P. James, N. Casillas, and W. H. Smyrl, *J. Electrochem. Soc.*, **143**, 3853 (1996).
6. M. Kozlowski, W. H. Smyrl, Lj. Atanasoska, and R. Atanasoski, *Electrochim. Acta*, **34**, 1763, (1989).
7. A. J. Bard, F. F. Fan, J. Kwak, and O. Lev, *Anal. Chem.*, **61**, 132 (1989).
8. M. A. Butler, *J. Electrochem. Soc.*, **130**, 2358 (1983).
9. M. A. Butler, *J. Electrochem. Soc.*, **131**, 2185 (1984).
10. D. R. Turner, U.S. Pat. 4,469,554 (1983).
11. L. F. Garfias-Mesias, M. Alodan, P. I. James, and W. H. Smyrl, *J. Electrochem. Soc.* **145**, 2005 (1998).
12. A. Szabo, *J. Phys. Chem.* **91**, 3108 (1987).
13. W. R. Smythe, *J. Appl. Phys.*, **22**, 1499 (1951).
14. G. I. Pennarun, C. Boxall, and D. O'Hare, *The Analyst*, **121**, 1779 (1996).

Linear Stability Analysis of Unsteady Galvanostatic Electrodeposition in the Two-Dimensional Diffusion-Limited Regime

J. Elezgaray, C. Léger, and F. Argoul*

Centre de Recherche Paul Pascal, 33600 Pessac, France

ABSTRACT

The nature and origin of the morphological instability which occurs in confined and unsupported electrodeposition experiments in galvanostatic regimes is discussed in terms of linear stability analysis, based on a theoretical work of Sundstrom and Bark.[1] The originality of our approach rests on the comparison of two-dimensional experimental concentration maps obtained by phase-shift interferometry with numerical simulations of the nonstationary evolution equations. We demonstrate both experimentally and theoretically that a morphological transition occurs when the concentration of reducible species approaches zero. We point out the relevance of the electroneutrality hypothesis for predicting the interfacial instability with reference to a destabilization mechanism, based on the existence of a space charge, proposed by Chazalviel.[2]

Introduction

The interpretation of the morphological instabilities[3] which can occur in an electrodeposition experiment has been the subject of constant interest during the last two decades.[1,4-6] All these studies are based on a linear stability analysis of the electrode planar interface inspired by Mullins and Sekerka's study of solidification.[7,8] Most of them are limited to stationary concentration fields and therefore are not likely to match the real situation in transitory processes. In that case, if we assume that the concentration field in front of the electrode is not stationary, in particular in quasi-semi-infinite cells, the linear stability analysis of the initial flat electrode must be assisted by numerical computations of the nonstationary concentration profiles prior to the instability.

The goal of this paper is the comparison of the electrode contours and concentration maps, as obtained by real-time phase shift interferometry[9] with the numerical prediction of a nonstationary linear stability analysis based on the stationary analysis of Sundstrom and Bark.[1] It is aimed at discussing the nature of the instability which occurs in confined galvanostatic electrodeposition experiments in unsupported electrolytes. In the second section we extract from the existing literature data the different approaches which have been devoted to linear stability analysis of galvanostatic electrodeposition processes and which have inspired this work. In the third section, we describe the electrochemical model and justify our nonstationary linear stability analysis. Our numerical simulations show that there are two regimes in the growth process. The first regime is dominated by a family of slowly growing modes, localized at rather larger scales, which does not significantly perturb the flat interface. Right before Sand's time[10] (when the interfacial concentration drops to zero), a second family of small-scale, fast-evolving modes appears, leading to ramified growth morphologies. We provide evidence for the occurrence of this instability at finite distance from Sand's time, i.e., for finite and nonnegligible interfacial concentration. We verify quantitatively the relevance of the electroneutrality assumption at that time (this fact is well admitted in presence of a supporting electrolyte) and we argue about the actual occurrence of a space charge[2] to explain the origin of the interfacial instability. In a fourth section we focus on the experimental analysis, based on phase-shift interferometry, and real-time recording of the shape of the electrode together with the voltage drop of our two-electrode cells. From the experimental data, we demonstrate that the instability of the interface occurs when the interfacial concentration approaches zero, which confirms our linear stability analysis.

* Electrochemical Society Active Member.